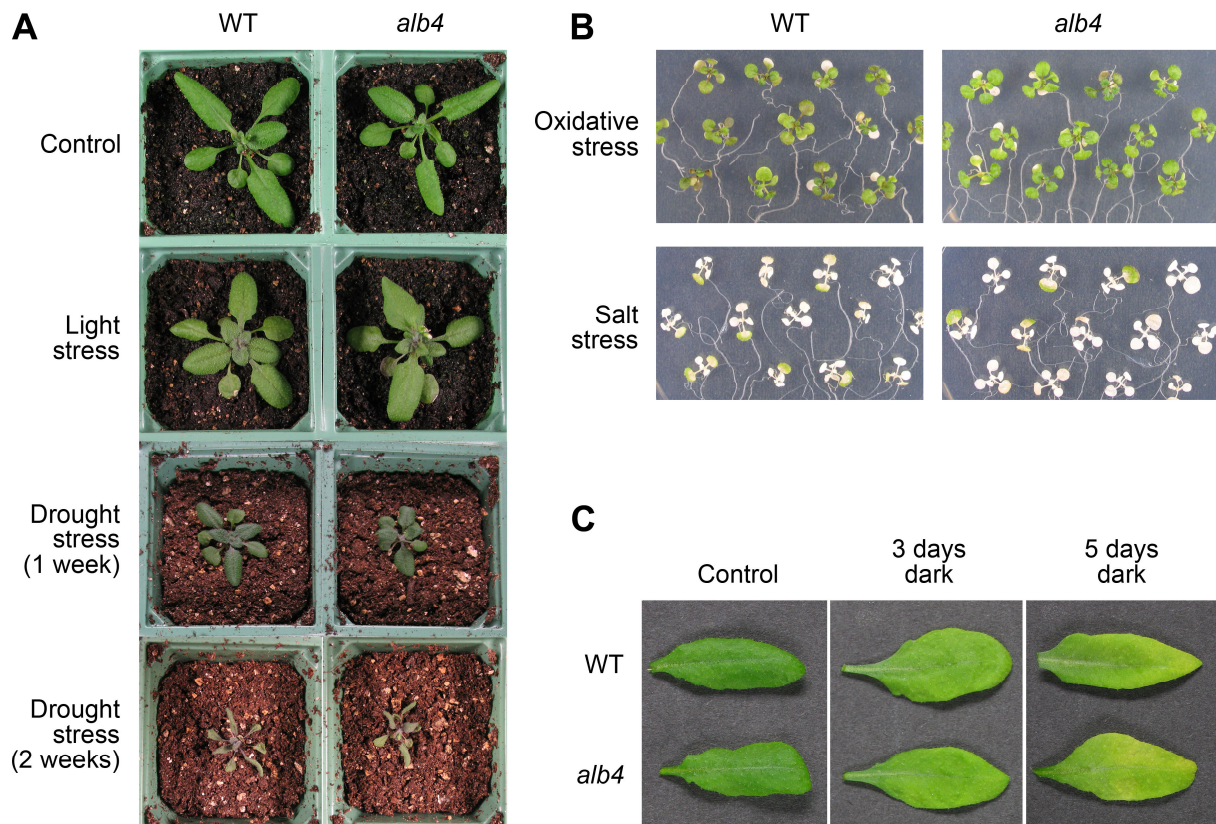
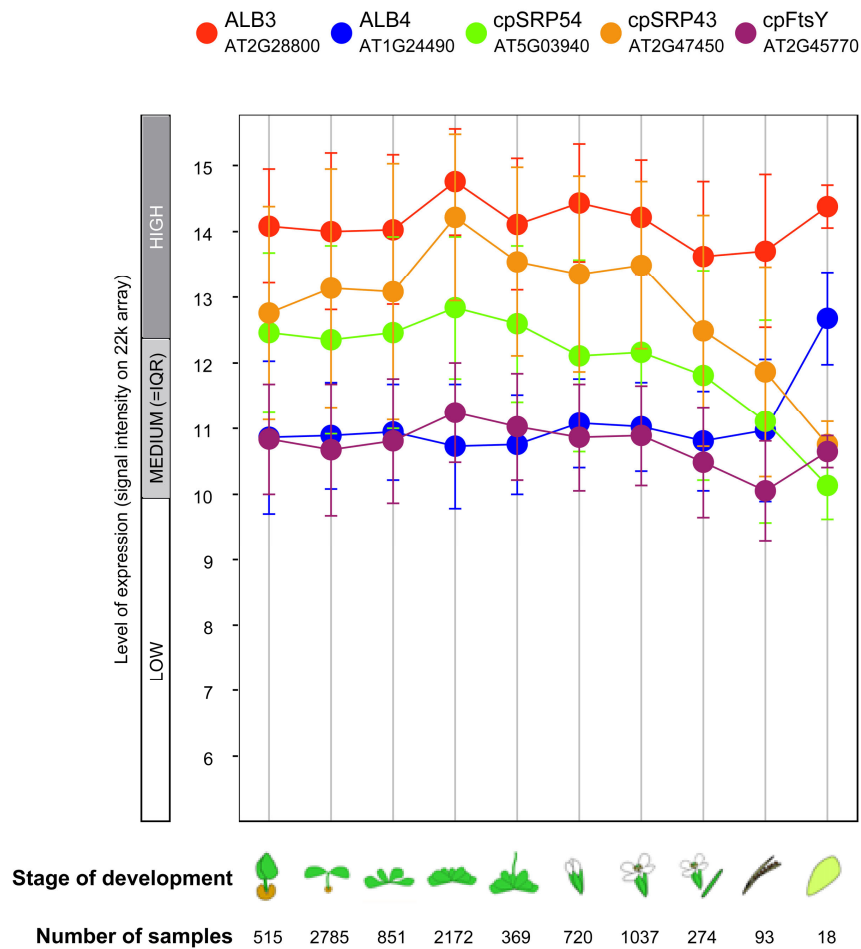


Supplemental Materials



Supplemental Figure S1. Phenotypic assessment of *alb4* mutant plants under different stress conditions.

(A) High-light stress and drought stress. Wild-type (WT) and *alb4* mutant plants were grown on soil under standard conditions (Control) for four weeks. For light stress, three-week-old plants were treated with 4 hours of 2000 $\mu\text{mol}/\text{m}^2/\text{s}$ high-intensity white light per day for one week. For drought stress, 3-week-old plants were withdrawn from watering for one and two weeks, as indicated. (B) Oxidative stress and salinity stress. For oxidative stress, two-week-old seedlings grown *in vitro* were transferred to MS medium containing 1 μM paraquat (PQ) and photographed after two weeks. For salt stress, two-week-old seedlings grown *in vitro* were transferred to MS medium containing 250 mM NaCl and photographed after 3 days. (C) Dark stress. To induce senescence, individual rosette leaves of 4-week-old plants were wrapped in aluminium foil and left for 3 or 5 days prior to photography. In all cases, the images shown are of representative plants or leaves.



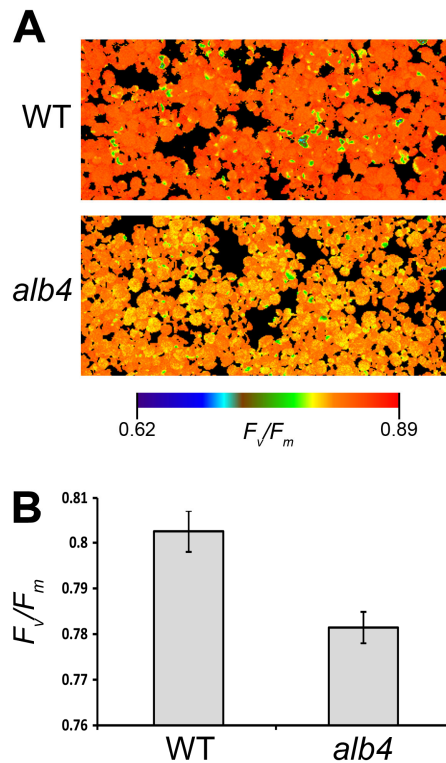
Supplemental Figure S2. Expression levels of genes relevant to this study as determined using public microarray data.

The expression levels of *ALB4* (AT1G24490) and of the components of the cpSRP pathway (*ALB3*, AT2G28800; *cpSRP54*, AT5G03940; *cpSRP43*, AT2G47450; and *cpFtsY*, AT2G45770) based on Affymetrix GeneChip data were compared using Genevestigator (<https://www.genevestigator.com>). Data from ATH arrays are shown in a scatter-plot diagram with the x-axis representing the following developmental stages, from left to right: germinating seed, seedling, young rosette, developed rosette, bolting, young flower, developed flower, flowers and siliques, mature siliques, and senescent leaves. For each developmental stage, the number of samples is indicated below the stage. The values in the plot represent means, and the error bars show standard errors. Medium expression levels are defined as the interquartile range (IQR) on the y-axis; values below the IQR are defined as “low expression” and values above the IQR as “high expression”.



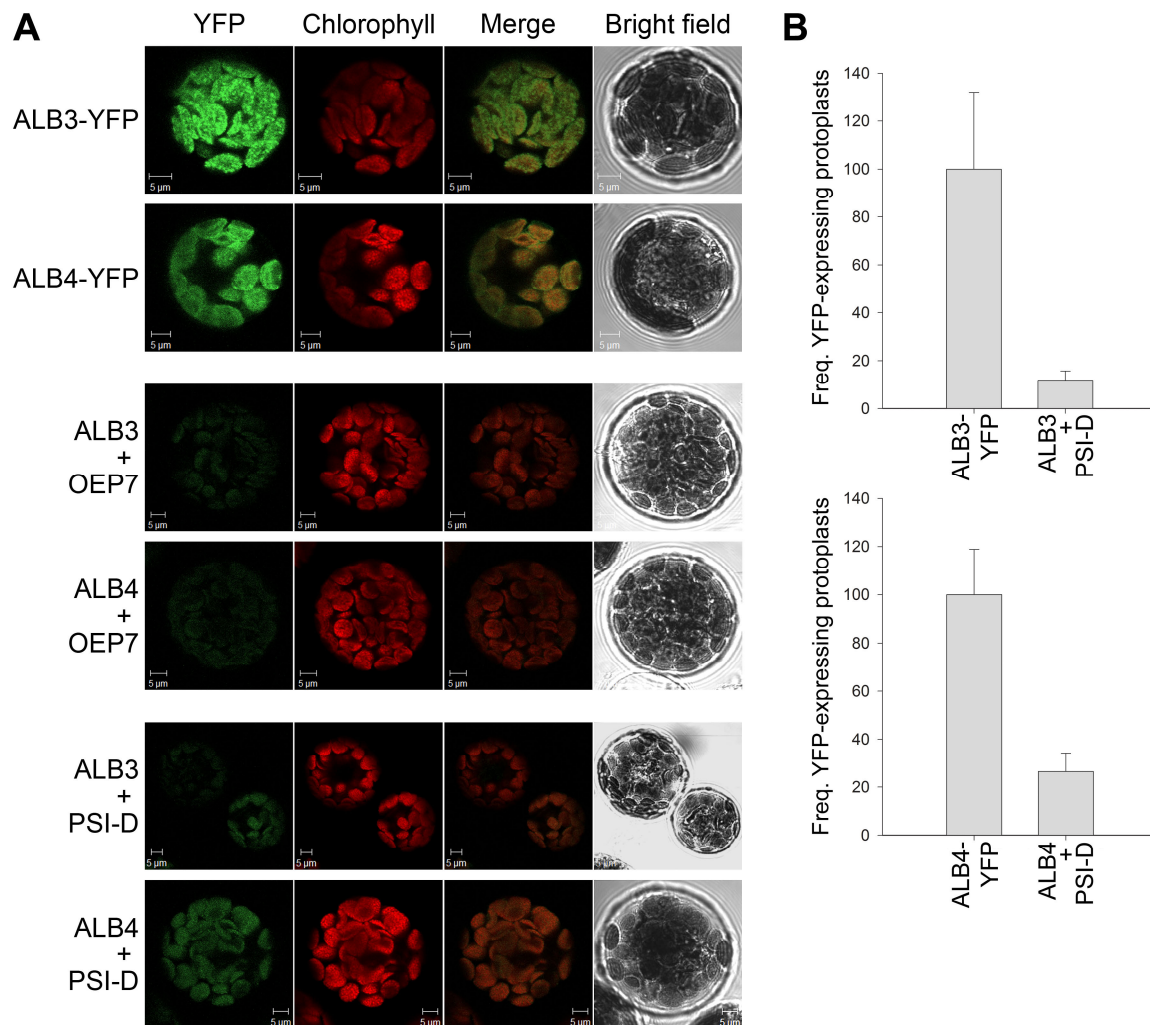
Supplemental Figure S3. Specificity analysis of the anti-ALB3 and anti-ALB4 antibodies.

Total protein extracts of wild type (WT), *alb4* and *alb3* plants were loaded according to equal total protein amount as determined by the Bradford assay and analysed by immunoblotting. The blotting membrane was cut into two identical halves, and one half was incubated with the anti-ALB3 antibody while the other half was incubated with the anti-ALB4 antibody. Images derived from each half, after development, are presented here in precise vertical alignment. The results show that the ALB3 and ALB4 proteins migrate at clearly different positions during electrophoresis. No band corresponding to the size of ALB4 (55 kDa) was detected with the anti-ALB3 antibody, showing that this antibody is specific. The anti-ALB4 antibody does detect a band (marked with an asterisk, *) that migrates close to the position of ALB3 (45 kDa). However, this band obviously does not result from cross-reaction of the ALB4 antibody with ALB3 because (a) it does not become weaker in the *alb3* mutant relative to wild type, and (b) it migrates at a slightly higher position. As this band is absent in the *alb4* mutant, it may in fact correspond to a truncated form of the ALB4 protein.



Supplemental Figure S4. Measurement of photosynthetic performance in the *alb4* mutant using a chlorophyll fluorescence imaging system.

Chlorophyll fluorescence imaging was employed to measure the maximum photochemical efficiency of photosystem II (F_v/F_m). Wild-type and *alb4* mutant seedlings, both 17 days old, were grown on half-strength MS agar plates supplemented with 0.5% sucrose and dark adapted for 1 hour before measurement. Representative images are shown (A); the coloured bar indicates the range of F_v/F_m values shown in the plant images. Mean F_v/F_m ratios were calculated based on 16 individual measurements of each genotype (B). Error bars denote standard errors.



Supplemental Figure S5. Control analyses for the BiFC study.

(A) Wild-type protoplasts were (co)transfected with the indicated constructs and analysed by confocal microscopy as in Figure 6. Very clear, thylakoid-localized YFP signals were detected when using the ALB3-YFP and ALB4-YFP constructs, as in Figure 6. In contrast, no YFP signals were detected in the control ALB3 + OEP7 and ALB4 + OEP7 BiFC analyses; OEP7 is an envelope protein not predicted to interact with the ALB proteins. We also conducted control BiFC analyses using a thylakoidal protein, PSI-D, which was selected on the basis of results in Figure 5 showing no interaction with ALB4. In this case, for both ALB3 + PSI-D and ALB4 + PSI-D, very weak YFP signals were detected in a small number of protoplasts. All control analyses were conducted in both orientations (nY vs. cY), with identical results, and representative images are shown. (B) The frequency of protoplasts displaying the weak YFP signal in the PSI-D BiFC experiments was quantified. Values were calculated and normalized as in Figure 6, and are representative of experiments conducted in both orientations. Errors bars denote standard deviations (n=3). We interpret the weak, low-frequency YFP signals seen in the PSI-D control BiFC experiments to be due to non-specific

interactions that occur as a result of the overexpression of the partners in a tightly constrained locality. The clear differences in brightness and frequency between these PSI-D results and those seen for ALB protein homo- and heterodimerization support the notion that the latter interactions are specific.

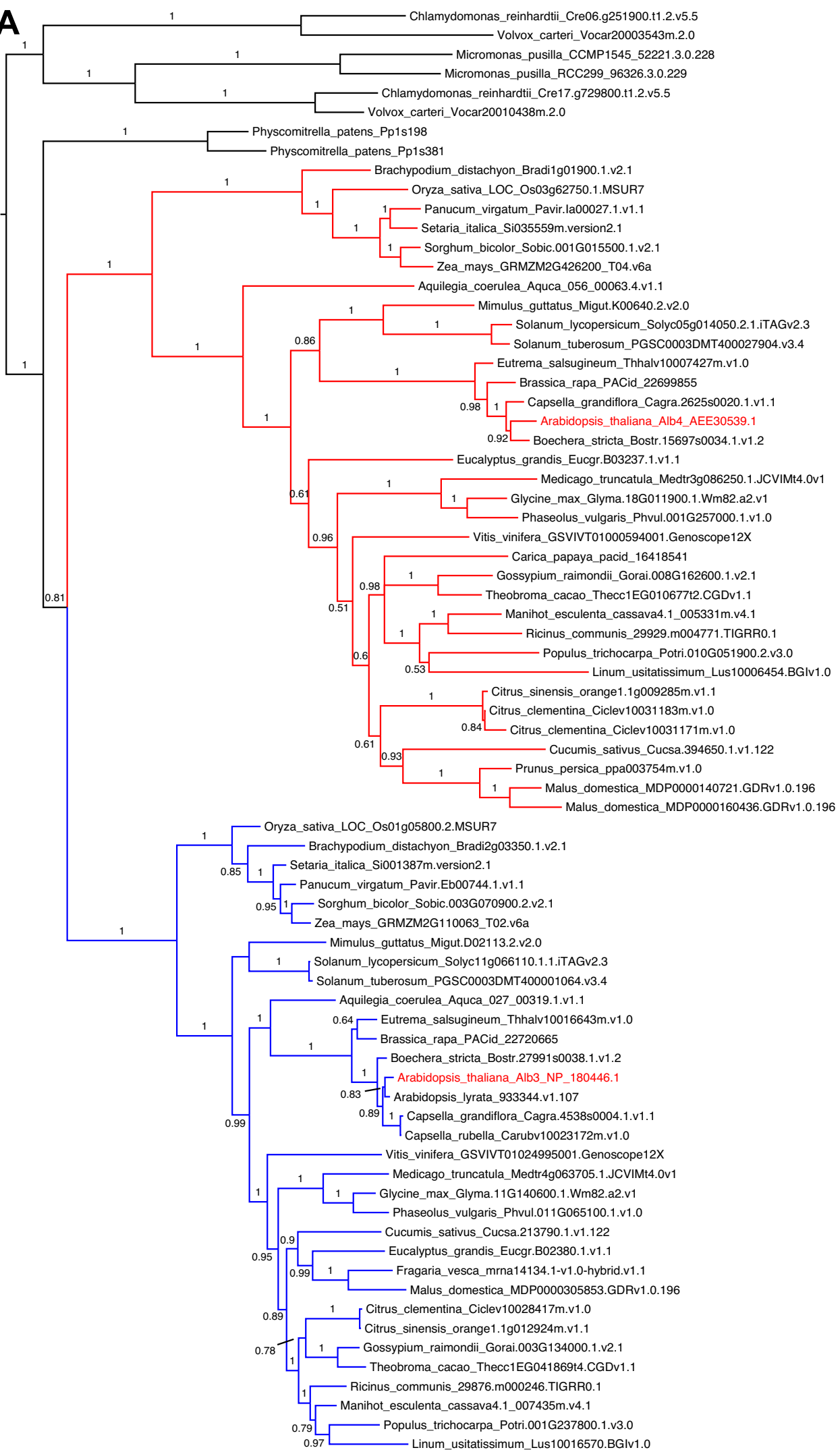
Supplemental Figure S6. Expanded phylogenetic analysis of ALB proteins and domains employing sequences from 39 different species.

Protein sequences of ALB3- (blue clade) and ALB4- (red clade) type proteins from a wide range of land plants were identified in the Phytozome database (v.10) and analysed phylogenetically as (A) full-length, (B) N-terminal, and (C) C-terminal datasets, using green algal sequences as the out-group. Indications of differences in evolutionary rate (i.e., differences in branch length between the red and blue clades) seen in A (full-length sequences) are not present in B (N-terminal sequences) but are strongly evident in C (C-terminal sequences). Thus, the analysis shows that accelerated evolution has occurred in the presumed protein-binding, C-terminal part of ALB4-type proteins. The scale bar below each tree indicates the number of expected changes per site along the branches, and posterior probability values are indicated at each branch. This expanded phylogenetic analysis of ALB sequences confirms the results presented in Figure 9.

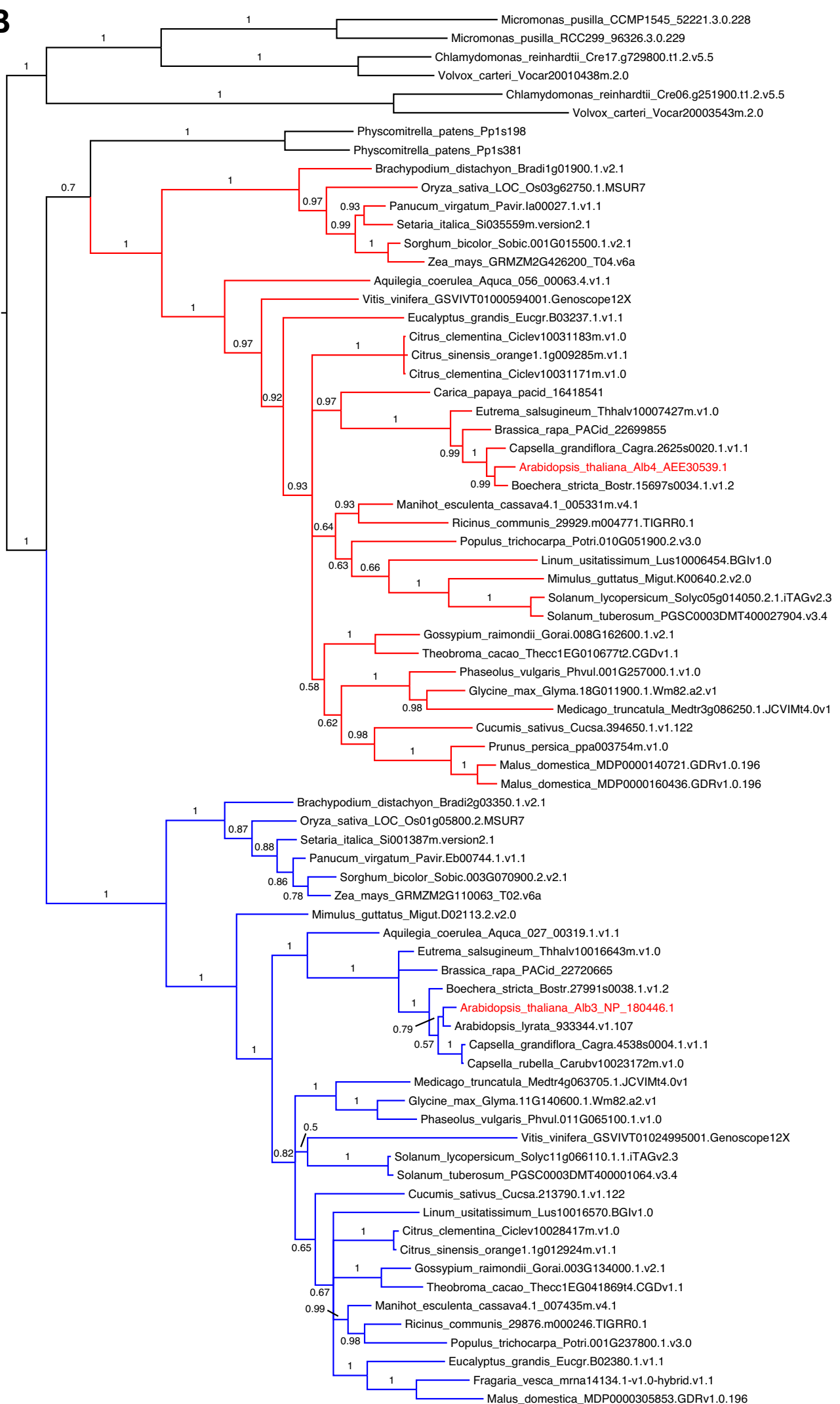
[See overleaf].

Supplemental Table S1. Sequences of the ALB proteins used in the phylogenetic analyses.

[See separate Excel file].

A

0.2

B

0.07

C